Rivista Italiana di Paleontologia e Stratigrafia	volume 115	no. 2	6 pls.	pp. 141-158	July 2009

FAMENNIAN CONODONTS FROM KAL-E-SARDAR SECTION, EASTERN TABAS, CENTRAL IRAN

HOSSEIN GHOLAMALIAN [1], MANSOUR GHORBANI [2] & SEYED-HADI SAJADI [3]

Received: November 24, 2008; accepted: May 28, 2009

Key words: Famennian, Conodonts, Kal-e-Sardar, Biostratigraphy, Biofacies.

Abstract. Sixty-three conodont species and subspecies from the Kal-e-Sardar section indicate that the strata span early to late Famennian. Contrary to most of the sections measured in the Shishtu Formation, the icriodid-polygnathid biofacies is restricted to the lower part of Kal-e-Sardar Famennian succession. Palmatolepid and bispathodid-dominated biofacies in the middle and upper part of section represent a deep shelf to mid-continental slope marine environment. The currently accepted ranges of *P. tichonovitchi, P. tenellus* and *P. inconcinnus* are early Famennian, late Frasnian-early Famennian, and early to middle Famennian, respectively, together with middle to late Famennian for *P. nodoundatus.* Two new species, *Polygnathus sardarensis* and *P. yazdii,* are proposed.

Riassunto. Sessantatre tra specie e sottospecie di conodonti sono state identificate nella sezione di Kal-e-Sardar entro la Formazione Shishtu, consentendo di riconoscere che la porzione studiata si estende dal Famenniano inferiore a quello superiore. A differenza di molte altre sezioni in questa parte della formazione la biofacies a icriodidi-polygnathidi è limitata alla parte inferiore della successione famenniana di Kal-e-Sardar. Nella parte media e superiore della sezione dominano invece le biofacies a palmatolepidi e bispathodidi, rappresentando un ambiente marino di piattaforma profonda o di pendio intracontinentale. Le distribuzioni attualmente accettate di *P. tichonovitchi, P. tenellus* e di *P. inconcinnus* sono rispettivamente Famenniano inferiore, tardo Frasniano-Famenniano inferiore, e Famenniano inferiore e medio. La distribuzione di *P. nodoundatus* è invece del Famenniano medio e superiore. Sono infine proposte due nuove specie, *Polygnathus sardarensis* e *P. yazdii.*

Introduction

The Kal-e-Sardar section near Niaz village, 23 km east of Tabas, is located along the northern side of the Sardar River, nearby the Nahrein dam (Figs 1, 2). Several individual exposures of Shishtu Formation are visible and the most complete succession is considered here (Hill IV of Becker et al. 2004). Coordinates of the studied section are N 33° 39′ 30.6″, E 57° 8′ 35.8″ (base) and N 33° 39′ 31.9″, E 57° 8′ 36″ (top).

Upper Devonian fossiliferous beds in the Kal-e-Sardar area have been examined by many researchers, with studies based on sparse conodont samples (Yazdi 1999; Ashouri 2002, 2004); goniatites (Walliser 1966; Ashouri & Yamini 2006), which includes the description of the Annulata Event on the basis of clymenids (Becker et al. 2004) and trilobites (Feist et al. 2003). Gholamalian (2007) identified the Frasnian-Famennian boundary by means of conodonts.

Abundant and diverse conodont faunas of 63 species and subspecies from 25 productive samples out of 29 allow correlation using the Upper Devonian conodont zonation of Ziegler (1962) and its more recent revision by Ziegler & Sandberg (1990).

Lithostratigraphy

The Shishtu Formation is the middle unit of the Ozbak-Kuh Group in the Shotori Range Mountains, eastern Tabas, east-central Iran (Fig. 2). Stöcklin et al. (1965) introduced the Kal-e-Sardar and southern Shotori Range successions as the reference sections of the Shishtu Formation. The Upper Devonian Shishtu 1 member is exposed in the small hills numbered from I to V by Becker et al. (2004) in the Kal-e-Sardar area on the northern side of Sardar River. Hill IV, with complete

1 Department of Geology, Faculty of Sciences, Hormozgan University, Bandar Abbas, I.R. Iran. E-mail: hossein.gholamalian@yahoo.com
2 Department of Geology, Faculty of Sciences, Hormozgan University, Bandar Abbas, I.R. Iran. E-mail: mmghorbanii@yahoo.de
3 Department of Geology, Islamic Azad University of Shiraz, Shiraz, I.R. Iran. E-mail: h_sajadi_fossil@yahoo.com

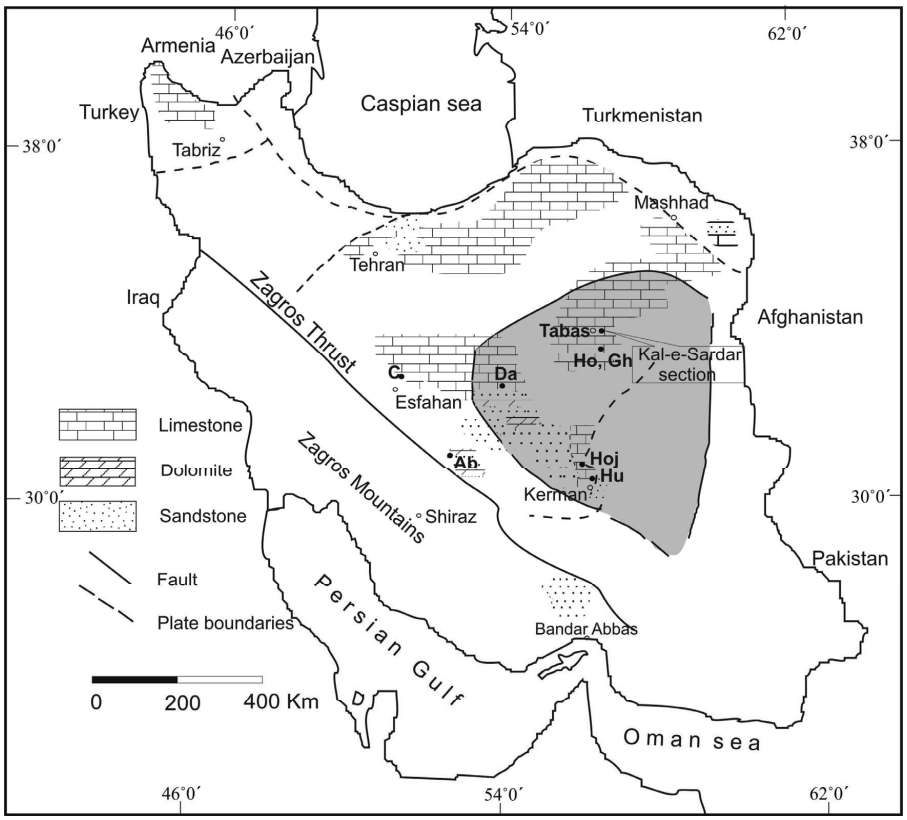

Fig. 1 - Late Devonian palaeogeographic map of Iran and the location of Kal-e-Sardar section. The map is redrawn form Wendt et al. (2005). The shaded area is east-central Iran microplate. Abbreviations used for localities are: C = Chahriseh, Da = Dalmeh, Ab = Abadeh, Hu = Hutk, Hoj = Hojedk, Ho = Howz-e-Dorah, and Gh = Ghale-Kalaghu.

undisturbed exposure of calcareous beds, was examined for this study.

In the Kal-e-Sardar section, the Famennian begins with 1.7 m of red ferruginous oolitic limestone that normally overlies the upper Frasnian black shales (Fig. 3). Gholamalian (2007) identified the Frasnian/Famennian boundary at the base of this oolitic limestone. The abrupt lithologic change from the upper Frasnian carbon rich shales of hypoxic/anoxic environment to the lower Famennian red oolitic limestones indicates a rapid marine regression at the end of Frasnian, corresponding to the Late Kellwasser Event (Gholamalian 2007, fig. 8). The succession continues with marls and alternations of oolitic and marly limestones. The middle part of the section is marked by a 10 cm bed of black fossiliferous marl (bed T2) which corresponds to the Annulata Event bed of Becker et al. (2004). This bed is conformably overlain by thin-bedded marly limestones and red oolitic limestones with two thin beds of sandy limestone at the base and top. 10.1 m of thin to medium-bedded marly limestones, two intercalations of thick-bedded limestones, and an oolitic interval overlie the lower layers and form the main part of succession (Fig. 3). Wendt et al. (2005, fig. 17) suggest that this forms a conformable Famennian-Tournaisian sequence, but on the contrary, the top of section appears to be overthrusted by upper Frasnian fossiliferous beds. Some conodont species such as *Polygnathus webbi, Icriodus alternatus alternatus* and *Ancyrodella buckyensis* were obtained from these beds.

Becker et al. (2004) described the strata of Hill IV and some of the other hills of Kal-e-Sardar area. They interpreted the differences between these sections by gravity tectonics and believe that Carboniferous displacement and redeposition of Famennian olistoliths was responsible for the mixing of Frasnian, Famennian and Carboniferous stratigraphic sequences. However, Wendt et al. (2005) do not agree with the redeposition interpretation. They consider that Alpine tectonic movements could account for the displacement of the successions. This seems a better explanation for thrusting of upper Frasnian beds over the top of upper Famennian.

There are significant lithologic and biofacies differences between the Upper Devonian sequences of Kal-e-Sardar and the southern Shotori Range sections at Howz-e-Dorah and Ghale-Kalaghu (Fig. 2) which cannot be attributed to post-Famennian gravity movements. These differences may be explained by horst – graben systems.

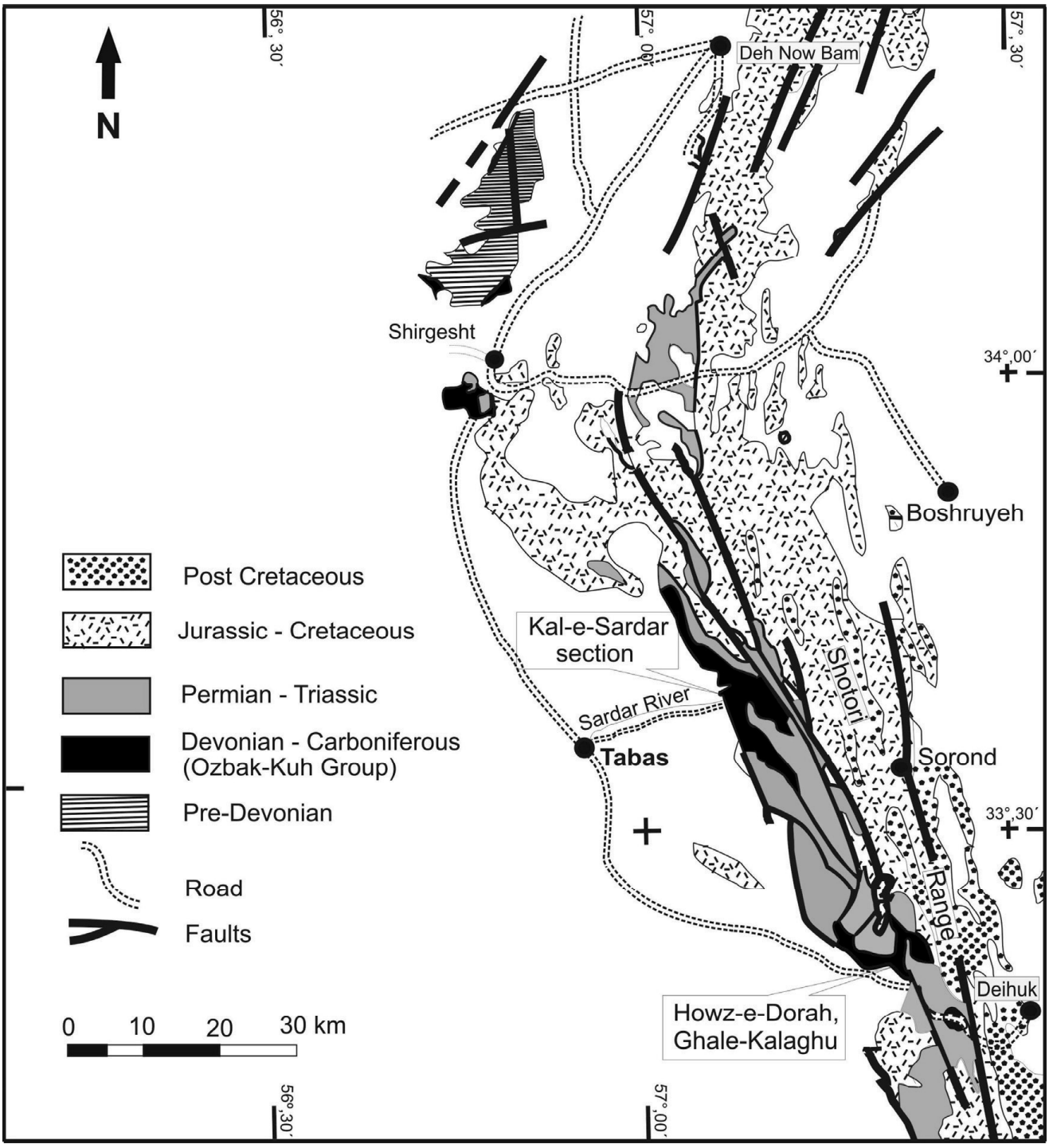

Fig. 2 - Geological map of Tabas area (after Stöcklin et al. 1965).

Biostratigraphy

Sixty-three conodont species and subspecies are clustered into nine conodont biozones (Tab. 1). Deep-water faunas in most parts of the section allow us to apply the palmatolepid zonation of Ziegler & Sandberg (1990), but owing to the lack of index palmatolepids in some cases, icriodid and polygnathid species are used to differentiate the upper and lower limits of zones (Pls. 1-6).

Lower to Middle *triangularis* zones (Bed H1). This interval can be recognized by the entry of *Palmatolepis triangularis* for the base and the entry of *Pal. tenuipunctata* in the next zone for the top. The fauna is associated with *Icriodus alternatus alternatus, Poly-*

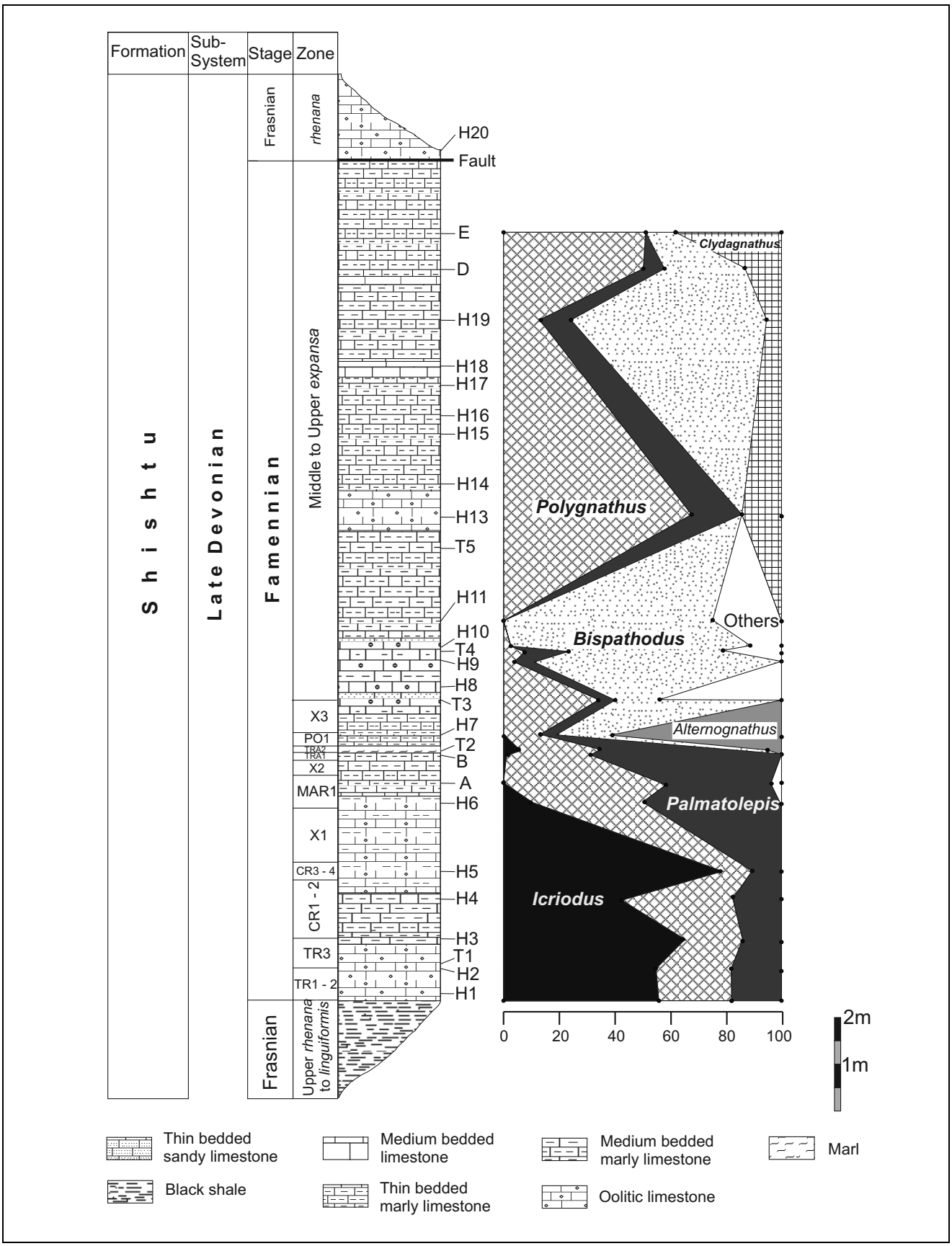

Fig. 3 - Stratigraphic column of Famennian strata and conodont biofacies curves in the Kal-e-Sardar section. Abbreviations used for biozones are: TR1 – 2 = Lower to Middle *triangularis* zones, TR3 = Upper *triangularis* Zone, CR1 – 2 = Lower to Middle *crepida* zones, CR3 – 4 = Upper to Uppermost *crepida* zones, MAR1 = Lower *marginifera* Zone, TRA1 = Lower *trachytera* Zone, TRA2 = Upper *trachytera* Zone PO1 = Lower *postera* Zone. Barren intervals: X1 =?Lower to Upper *rhomboidea* Zone, X2 = Upper to Uppermost *marginifera* zones, X3 = Upper *postera* to Lower *expansa* zones.

Zones	TR1-2	TR3	CR1-2		CR3-4	MAR1		TRA1	TRA2	PO1	Middle to Upper *expansa*														
Species \ Samples	H1	H2	H3	H4	H5	H6	A	B	T2	H7	T3	H8	H9	T4	H10	H11	T5	H13	H15	H16	H17	H18	H19	D	E
Pal. triangularis	3	30	13																						
Pal. tenuipunctata		1			5																				
P. lanceolus		14	4																						
P. tenellus	1	4	4																						
P. ratebi		4																							
P. communis group		3	5		2	14	7		1		7			5	1										2
P. brevilaminus	3	5	4	7	5																				
P. tichonovitchi		1																							
P. yazdii n. sp.		14				3		2																	
I. alternatus alternatus	9	55	20	48	50																				
I. alternatus mawsonae		30	50	14	11																				
I. iowaensis iowaensis		1			5																				
Pal. minuta loba			5	14																					
Pal. minuta minuta				5	1	16	1																		
Pal. quadrantinodosalobata				4																					
Pal. clarki				2																					
I. alternatus helmsi			6																						
Pal. subperlobata				1																					
P. nodocostatus			5	1	2	17	5	7	8	3															
P. pseudobrevilaminus				3		1																			
P. sardarensis n. sp.			8	47		2	2																		
Pal. perlobata schindewolfi					2	8	17	64	21					1				1	7		2	1	8		
Pal. crepida					3																				
P. glaber medius						2	14																		
Pal. quadrantinodosa quad.						1	1																		
Pal. quad. inflexoidea						3																			
Pal. quad. inflexa						1																			
Pal. glabra distorta							10	7																	
Pal. glabra glabra						6	1																		
Pal. glabra pectinata						20	12																		
Pal. glabra prima							2																		
Pal. gracilis gracilis							2		1		2	1	2	5										1	
P. inconcinnus							5	8																	
P. planirostratus							3																		
P. lagowiensis						7	10																		
P. aff. *lagowiensis*							2																		
P. nodoundatus							15	1	4								2	5							
I. aff. *iowaensis*						1																			
P. subirregularis								4	3																
P. glaber bilobatus								7																	
P. perplexus								6		2					1			5				1		2	1
Pal. gracilis sigmoidalis									1	1		1	1	6											
I. cornutus		9	28		8	10		1	3																
I. cf. *cornutus*									1																
Pal. rugosa cf. *ampla*									6																
Bi. stabilis									12	8	5	2		6		7	4				2		58	4	4
Alternognathus beulensis									4	30															
Bi. aculeatus aculeatus											1	1	26	35	45	156	3								
Bi. costatus													16		35	14									
P. semicostatus			4				2		1		5		1					4	1	3	1	2	7	4	14
P. delicatulus													1								2		4		
Pal. per. cf. *schindewolfi*																		1							
Pal. rugosa ampla																		2		1	1	2			
Ps. primus																59									
Ps. brevipennatus											1														
Ps. sp.										1	1														
P. sp.A				1																					
P. sp. B					1																				
P. sp. C					1													1							
Clydagnathus sp.																		3	2		1		5	2	12
Pel. inclinatus											1														
Branmehla inornata											6	2			10										1
Mehlina sp.							3				10			16					2						
Unassigned elements	1	110	98	76	8	330	140	112	152	6	8	3	7	59	111	203	44	49	69	56	12	46	139	26	41
Total	17	281	254	223	104	442	254	219	218	51	47	10	54	133	203	439	53	71	81	60	21	52	221	39	75

Tab. 1 - Range chart of Famennian conodonts in the Kal-e-Sardar section. Arrows show the first and last appearance datums. See Fig. 3 for explanation of biozones.

gnathus brevilaminus and *P. tenellus.* According to Ziegler & Sandberg (1990) and Klapper et al. (1993), the Frasnian-Famennian boundary is located at the base of the Lower *triangularis* Zone with the first specimens of *Pal. triangularis*. Klapper et al. (2004) and Klapper (2007) believe that the first appearance of *Pal. triangularis* occurs slightly above the base of the Lower *triangularis* Zone in European reference sections. On the other hand, more precise reidentification of figure 9L of Gholamalian (2007) shows the presence of *Pal. subperlobata.* Its lowest occurrence can characterize the Lower *triangularis* Zone (Klapper et al. 2004). Recovery of the first specimens of *Pal. triangularis* from bed H1 in the present study confirms the identification of the F-F boundary by Gholamalian (2007, fig. 6).

Upper *triangularis* zones (Bed H2). The association of *Icriodus alternatus alternatus, I. alternatus mawsonae, I. cornutus, I. iowaensis iowaensis, Palmatolepis triangularis, Pal. tenuipunctata, Polygnathus lanceolus, P. communis* group, *P. brevilaminus, P. ratebi, P. tenellus, P. tichonovitchi* and *P. yazdii* n. sp. can be seen here. The boundaries are identified by the entry of *Pal. tenuipunctata* for the base and the entry of *Pal. minuta loba* and *Pal. quadrantinodosalobata* in the next zone for the top. *Polygnathus lanceolus,* which ranges from Upper *triangularis* to Uppermost *crepida* zones, occurs in this interval. *Polygnathus tichonovitchi,* which was previously reported by Kuzmin & Melnikova (1991) from the *crepida* Zone, makes its first appearance here.

Lower to Middle *crepida* zones (Beds H3-H4). The lower limit of this interval is recognized by the first appearance datum of *Palmatolepis minuta loba* and the presence of *Pal. quadrantinodosalobata.* The upper limit can be identified by the last presence of *Pal. clarki* ranging from Upper *triangularis* to Middle *crepida* zones (Schülke 1995). Entry of *Pal. perlobata schindewolfi* at the base of the next zone can also determine the top of this interval. Other associated fauna are *Icriodus alternatus alternatus, I. alternatus mawsonae, I. alternatus helmsi, I. cornutus, Pal. minuta minuta, Pal. subperlobata, Pal. triangularis, Polygnathus brevilaminus, P. communis* group, *P. nodocostatus, P. lanceolus, P. tenellus, P. semicostatus, P. pseudobrevilaminus, P. sardarensis* n. sp., and *P.* sp. A. Ji & Ziegler (1993) proposed to limit the age of *P. tenellus* to Lower *rhenana*-Lower *triangularis* zones, but its last appearance datum is within this interval.

Upper to Uppermost *crepida* zones (Bed H5). The lower limit is identified by the entry of *Palmatolepis perlobata schindewolfi*, the upper one by the last occurrence of *Pal. tenuipunctata* ranging from Upper *triangularis* to Uppermost *crepida* zones (Ji & Ziegler 1993). *Palmatolepis crepida* that ranges from Lower *crepida to* Lower *rhomboidea* zones occurs here. The final occurrence of specimens of *Icriodus alternatus alternatus* and *I. alternatus mawsonae* is found in this interval. Other taxa of this zone are: *I. cornutus, I. iowaensis iowaensis, Pal. minuta minuta, Polygnathus brevilaminus, P. communis* group, *P. nodocostatus, P.* sp. B.

Lower *marginifera* Zone (Beds H6-A). The lower boundary of this zone is determined by the entry of *Polygnathus glaber medius*. The upper limit can be identified by the last occurrence of *Pal. quadrantinodosa quadrantinodosa,* which is restricted to the upper part of Upper *rhomboidea*-Lower *marginifera* zones (Ziegler & Sandberg 1984, fig. 2; Capkinoglu 1997). *Palmatolepis quadrantinodosa inflexa,* ranging from Upper *rhomboidea* to Lower *marginifera* zones and *Pal. glabra distorta* (Lower *marginifera*-Lower *trachytera* zones) are important taxa in this interval (Ji & Ziegler 1993; Barskov et al. 1987). *Polygnathus lagowiensis,* with a range from Lower *rhomboidea* to Upper *marginifera* zones (Helms & Wolska 1967), occurs here. Perri & Spalletta (1990) restricted the range of *P. nodoundatus* to Upper *marginifera*-Lower *trachytera* zones. However, the species enters in the present interval, indicating a longer range, from Lower *marginifera* to Upper *expansa* zones.

Other associated conodont fauna are: *Palmatolepis glabra pectinata, Pal. minuta minuta, Pal. perlobata schindewolfi, Pal. glabra glabra, Pal. glabra prima, Pal. gracilis gracilis Polygnathus communis* group, *P. semicostatus, P. planirostartus, P. inconcinnus, P. nodocostatus, P. pseudobrevilaminus, P.* aff. *lagowiensis, P. sardarensis* n. sp., *P. yazdii* n. sp., *Icriodus cornutus*, *I.* aff. *iowaensis, Mehlina* sp.

Lower *trachytera* Zone (Bed B). The base of this zone can be discriminated by the entry of *P. subirregularis*, the top by the last appearance datum of *Pal. glabra distorta*. The final occurrence of *Polygnathus glaber bilobatus,* ranging the Upper *marginifera*-Lower *trachytera* zones (Perri & Spalletta 1990), may also used to determine the upper limit of this zone. *Polygnathus inconcinnus* is known from Upper *triangularis* to Upper *crepida* zones (Kuzmin & Melnikova 1991), but its last appearance datum occurs here and its new range is here proposed from Upper *triangularis* to Lower *trachytera* zones. Other associated species are: *Palmatolepis perlobata schindewolfi, P. nodocostatus, P. nodoundatus, P. perplexus, P. yazdii* n. sp., *I. cornutus.*

Upper *trachytera* Zone (Bed T2). The base of this biozone can be recognized by the first appearance of *Palmatolepis gracilis sigmoidalis,* which ranges from Upper *trachytera* to ?Upper *praesulcata* zones (Ji &

Ziegler 1993). The top of this zone can be identified by last appearance of *Icriodus cornutus* (Sandberg & Dreesen 1984). Other fauna are: *Bispathodus stabilis, Palmatolepis gracilis gracilis, Pal. rugosa* cf. *ampla, Pal. perlobata schindewolfi, Polygnathus communis* group, *P. nodocostatus, P. nodoundatus, P. semicostatus, P. subirregularis, Alternognathus beulensis, I.* cf. *cornutus.* The Annulata Event bed (M) of Becker et al. (2004) is the same as bed T2, which is within the Upper *trachytera* Zone.

Lower *postera* zones (Bed H7). The base of this interval is coincident to the last appearance of *Icriodus cornutus* at the top of the previous zone. The top of the interval is known by the last appearance datum of *Alternognathus beulensis,* which ranges from Uppermost *marginifera* to Lower *postera* zones (Zigler & Sandberg 1984). *Bispathodus stabilis, Palmatolepis gracilis sigmoidalis, Pal. perlobata schindewolfi, Polygnathus communis* group, *P. nodocostatus, P. semicostatus, P. subirregularis, P. perplexus,* and *Pseudopolygnathus* sp. are associated species.

Middle to Upper *expansa* zones (Beds T3-E). The entry of *Bispathodus aculeatus aculeatus,* which ranges from Middle *expansa* to Upper *crenulata* zones (Ziegler et al. 1974), defines the base of this interval. *Polygnathus semicostatus,* which ranges from Middle *crepida* to Upper *expansa* zones, terminates this interval. Associated species are: *Bispathodus costatus, Bi. stabilis, Palmatolepis gracilis gracilis, Pal. gracilis sigmoidalis, Pal. perlobata schindewolfi, Pal. perlobata* cf. *schindewolfi, Pal. rugosa ampla, P. delicatulus, P. communis* group, *P. nodocostatus, P. nodoundatus, P. perplexus, P.* sp. C, *P. yazdii* n. sp., *Pseudopolygnathus primus, Ps. brevipennatus, Ps.* sp., *Clydagnathus* sp., *Mehlina* sp., *Branmehla inornata, Pelekysgnathus inclinatus.*

Barren intervals. There are three intervals which do not yield any conodont specimen, so the ages of these beds have been recognized on the basis of their stratigraphic position. The intervals are: X1 =?Lower to Upper *rhomboidea*, X2 =?Upper to Uppermost *marginifera*, X3 =?Upper *postera* to Lower *expansa* (Fig. 3).

Biofacies and sea level changes

This palaeoenvironmental and palaeoecological investigation is based on field observations and statistical data. Biofacies quantitative analyses are erected on the basis of concepts of Pohler & Barnes (1990). The biofacies of the studied section is compared with the models of Sandberg & Dreesen (1984), Sandberg et al. (1988) and Savoy & Harris (1993). Abundance of *Icriodus* with absence or rare occurrence of deep marine genera such as *Palmatolepis* is typical of most central Iran sequences: e.g. Howz-e-Dorah (Southern Shotori Range); Abadeh; Hutk and Hojedk (Kerman); and Chahriseh (Esfahan) (Yazdi et al. 2000; Wendt et al. 2002, 2005; Gholamalian 2006, 2007; Gholamalian & Kebriaei 2008). The Kal-e-Sardar section beds are rich in *Palmatolepis* and some other deep marine genera.

After the sea level rise in the late Frasnian (Upper *rhenana-linguiformis* zones) of the Kal-e-Sardar section, the spreading of the icriodid-polygnathid biofacies indicates a rapid eustatic shallowing at the base of the Lower *triangularis* Zone (Gholamalian 2007). This is similar to the inner shelf environment of the White Horse Pass section of Nevada (Sandberg et al. 1988). This situation continues to the Middle *crepida* Zone (Fig. 3). The increase of icriodid specimens in the Upper to Uppermost *crepida* zones indicates a shallower environment. The palmatolepid-polygnathid biofacies then appears in the Lower *marginifera* zone and continues to the Upper *trachytera* zone (Tab. 2). This biofacies represents a sea level rise and indicates a deep shelf to mid-continental slope environment, similar to that of the Alberta Platform (Savoy & Harris 1993, fig. 11A). The Upper *trachytera* Zone (Bed T2) shows the maximum sea level high-standing during the Annulata Event, whereas the overlying Lower *postera* zone (bed H7) with 65% of *Alternognathus,* indicative of a sub-

Zones	TR1-2	TR3	CR1-2		CR3-4	MAR1		TRA1	TRA2	PO1	Middle to Upper *expansa*														
% \ Sample	H1	H2	H3	H4	H5	H6	A	B	T2	H7	T3	H8	H9	T4	H10	H11	T5	H13	H15	H16	H17	H18	H19	D	E
% *Icriodus*	57	56	65	42	78	10		1	5																
% *Polygnathus*	25	26	22	40	11	40	57	30	30	13	34		4	7	2			68					13	50	51
% *Palmatolepis*	18	18	12	18	11	50	41	69	41	4	6		6	16				18					10	8	
% *Bispathodus*									17	17	16		90	56	87	75							71	28	12
%*Clydagnathus*																		14					6	14	36
%*Alternognathus*									5	65															
Others							2				44			22	11	25									
Biofacies	I-P	I-P	I-P	I-P	I	Pal-P	P-Pal	Pal-P	Pal-P		P-Bi		Bi	Bi	Bi	Bi		P-Pal					Bi	P-Bi	P-Cl

Tab. 2 - Biofacies chart of Famennian conodonts from Kal-e-Sardar section. See Fig. 3 for explanation of biozones.

tidal environment (Ziegler & Sandberg 1984, p. 185), shows an abrupt sea level fall (Fig. 3).

The polygnathid-bispathodid facies occurs at the base of Middle to Upper *expansa* zones (bed T3). The assemblages of beds H9 to D change to bispathodid, bispathodid-polygnathid and polygnathid-palmatolepid biofacies, which indicate a deep shelf environment. The final bed (E), with a mixed polygnathid-clydagnathid biofacies, may represent a shallow near-shore marine environment (Tab. 2).

The biofacies of the lower part of the Famennian sequence of Kal-e-Sardar is very similar to that of Kerman (Hutk and Hojedk) and Dalmeh sections (Hairapetian & Yazdi 2003; Gholamalian 2006; Gholamalian & Kebriaei 2008). The icriodid-polygnathid and icriodid biofacies indicate the predominance of shallow subtidal environments in the early Famennian (Lower *triangularis* to Uppermost *crepida* zones) of central Iran. The icriodid-polygnathid biofacies of southern Shotori Range sections (Howz-e-Dorah and Ghale-Kalaghu) appears in the Lower *crepida* Zone after *triangularis* Zone non-marine deposition (Gholamalian 2007). Predominance of palmatolepid-polygnathid, bispathodid, and polygnathid-bispathodid biofacies in the Lower *marginifera* to Upper *expansa* zones cannot be observed in most of Iranian sequences except for the Kal-e-Sardar section. Middle and Upper Famennian beds of some sections, e.g. Howz-e-Dorah, show predominance of icriodid and icriodid-polygnathid facies. Equivalent beds in the Hutk area are restricted to 41.4 m of offshore sandstones (Gholamalian 2006). By contrast, subsequent beds in the Kal-e-Sardar section have palmatolepid-polgnathid and polygnathid-bispathodid biofacies. These significant differences can be explained by the activity of large north-south trending faults which formed graben systems in which deeper marine environments developed and deep marine sediments were deposited. The erosion of the upper part of upper Frasnian strata and *triangularis* Zone none-marine depositions of southern Shotori Range sections against the upper Frasnian black shales and lower Famennian marine limestones of Kal-e-Sardar section are evidence of tectonic activity during late Frasnian and early Famennian. Such activity resulted in a deep sedimentary environment for most of the Famennian sequence of Kal-e-Sardar, as shown by the pelagic biofacies. On the other hand, the thickness of the Kal-e-Sardar Famennian sequence is considerably thinner than equivalent strata in Iran: 23 m as against tens of meters in Howz-e-Dorah and hundreds of meters in the Chahriseh and Dalmeh sections (Yazdi 1999; Hairapetian & Yazdi 2003; Gholamalian 2007). The reduced thickness and pelagic fauna indicate that the studied sequence is a condensed section. Sedimentation rate in the lower part of the section was very slow, especially in the Lower *marginifera* to Lower *postera* zones. It increased in the Middle to Upper *expansa* zones, but this rate is still very much slower than that of other Iranian sequences (e.g. Chahriseh and Dalmeh).

Systematic Palaeontology

Order **Ozarkodinida** Dzik, 1976

Family Polygnathidae Bassler, 1925

Genus *Polygnathus* Hinde, 1879

Type species: *Polygnathus dubius* Hinde, 1879

Polygnathus sardarensis n. sp.

Pl. 5, Figs 1-16

1990 *Polygnathus granulosus* Branson & Mehl - Perri & Spalletta, Pl. 5, Figs 5a-5b.

Holotype: HUIC339, sample H4, Kal-e-Sardar section, Plate 5, Figs 5-7.

Paratype: HUIC337, sample H4, Kal-e-Sardar section, Plate 5, Figs 1-2.

Material: 8 specimens from sample H3, 47 from H4, 2 from H6 and 2 from A, Kal-e-Sardar section.

Etymology: Sardar is the name a river that flows in Tabas.

Diagnosis: A polygnathid species with platform surface completely covered by nodes, high and fused carina reaching the posterior tip. The free blade is high and denticulated.

Description. Pa elements of this species are more or less symmetric. Platform is leaf-like to elliptical in outline. The platform is widest in the middle and gradually becomes narrower towards the posterior end to form a sharp posterior tip. Coarse nodes randomly cover the entire platform surface. The carina is high, composed of fused denticles and reaches the posterior tip. The free blade is composed of 5-6 high isometric denticles and equal to two-thirds of platform length. A narrow basal cavity with small flanks is located beneath the anterior quarter of the platform. The keel is distinct.

Remarks. *Polygnathus sardarensis* can be distinguished from *P. lagowiensis* by having coarser nodes on the platform, and by the isometric denticles of the free blade. *Polygnathus sardarensis* has a higher carina, composed of fused denticles and reaches the posterior tip, whereas *P. lagowiensis* is characterized by small nodes on the platform and separated denticles on the carina. *Polygnathus granulosus* can be discriminated from *P. sardarensis* by the absence of nodes on the anterior quarter of the platform surface and a basal cavity without flanks (Barskov et al. 1991, pl. 25, figs 1a-2).

Range. Lower *crepida* - Lower *marginifera* zones (Tab. 1).

Polygnathus yazdii n. sp.

Pl. 4, Figs 18-23, 25

Holotype: HUIC331, sample H2, Kal-e-Sardar section, Plate 4, Figs 18-20.

Paratype: HUIC334, sample B, Kal-e-Sardar section, Plate 4, Figs 21-23.

Material: 14 specimens from sample H2, 3 from H6, 2 from B, Kal-e-Sardar section.

Etymology: In honor of Iranian conodont researcher Dr. Mehdi Yazdi (Esfahan University).

Diagnosis: A polygnathid species with slightly asymmetric platform, one longitudinal ridge on each side of carina, and small basal cavity that is located on the anteriormost part of element.

Description. Pa elements of *Polygnathus yazdii* are slightly asymmetric. The platform is slightly wider at mid-length than the anterior part and makes a weak lobe. It becomes narrower toward the posterior end and forms a sharp tip. Carina is high, well fused, reaches the posterior end, and is composed of small separated nodes. Two nodose fused longitudinal ridges are parallel to the carina. The free blade equals one-third of the complete element and is composed of denticles which reduce in height posterior-wards. The platform is slightly curved downwards. The basal cavity is small and located beneath the anterior quarter of the platform.

Remarks. *Polygnathus inconcinnus* can be recognized from *P. yazdii* by having a shorter free blade with the highest denticle at the junction to the platform and the location of the basal cavity that impends to the centre (anterior one-third) of the platform. A laterally arched and more downwards platform is the other characteristic of *P. inconcinnus*.

Polygnathus nodoundatus differs from *P. yazdii* by a broader platform and a carina that becomes weak towards the posterior end as well as two longitudinal ridges which are restricted to the anterior part of the platform.

Range. By considering the association with index species, *Polygnathus yazdii* has the range of Upper *triangularis*-Lower *trachytera* zones.

Conclusions

Beside the conodont communities in the Lower *triangularis* to Uppermost *crepida* zones typical of an inner shelf environment, Lower *marginifera* to Upper *trachytera* zones show a marine sea level rise. Rapidly shallowing conditions appear at the base of the Lower *postera* zone bed (H7) that overlies the Annulata Event bed (T2). Open marine environments occurred again in the Middle to Upper *expansa* zones.

Polygnathus sardarensis n. sp. with the range of Lower *crepida*-Lower *trachytera* zones and *P. yazdii* n. sp. ranging Upper *triangularis*-Lower *trachytera* zones are introduced. New ranges are proposed for some known species: Upper *triangularis* to Upper *crepida*, zones, Lower *rhenana* to Middle *crepida* zones, and Upper *triangularis* to Lower *trachytera* zones for *P. tichonovitchi*, *P. tenellus* and *P. inconcinnus* respectively. Lower *marginifera* to Upper *expansa* zones is new range of *P. nodoundatus*.

Acknowledgements. Authors are grateful for all of helps from Dr. A.R. Ashouri and Ms. Sadeghi, Ferdowsi University of Mashhad, central laboratory for SEM micrographs. Our sincere thanks go to Latha Menon (Oxford) and Vachik Hairapetian (Esfahan), who made linguistic corrections and useful comments. Authors express sincerely gratitude to Carlo Corradini, Hanna Matyja and D.J. Over for their critical comments on the early version of manuscript.

PLATE 1

All figures are x 35

Figs. 1-3 *Icriodus alternatus alternatus* Branson & Mehl, 1934: 1) upper view of HUIC 219, sample H1; 2) upper view of HUIC 220, sample H2; 3) upper view of HUIC 221, sample H2.

Fig. 4 *Icriodus alternatus helmsi* Sandberg & Dreesen, 1984: upper view of HUIC 222, sample H3.

Fig. 5 *Icriodus alternatus mawsonae* Yazdi, 1999: upper view of HUIC 223, sample H2.

Fig. 6 *Icriodus* cf. *cornutus* Sannemann, 1955: upper view of HUIC 225, sample T2.

Figs. 7-9 *Icriodus cornutus* Sannemann, 1955: 7) upper view of HUIC 226, sample H2; 8-9) lateral and upper view of HUIC 227, sample H3.

Fig. 10 *Icriodus* aff. *iowaensis* Youngquist & Peterson, 1947: upper view of HUIC 233, sample H6.

Fig. 11 *Icriodus iowaensis iowaensis* Youngquist & Peterson, 1947: upper view of HUIC 234, sample H5.

Figs. 12-14 *Palmatolepis minuta minuta* Branson & Mehl, 1934: 12) upper view of HUIC 258, sample H9; 13) upper view of HUIC 257, sample H6;14) upper view of HUIC 259, sample H10.

Fig. 15 *Palmatolepis quadrantinodosa quadrantinodosa* Branson & Mehl, 1934: upper view of HUIC 260, sample H6.

Fig. 16 *Palmatolepis quadrantinodosa inflexoidea* Ziegler, 1962: upper view of HUIC 293, sample H6.

Figs. 17, 20-21 *Palmatolepis minuta loba* Helms, 1963: 17) upper view of HUIC 262, sample H4; 20) upper view of HUIC 261, sample T2; 21) upper view of HUIC 265, sample H4.

Figs. 18-19 *Palmatolepis clarki* Ziegler, 1962: 19) upper view of HUIC 263, sample H4; 20) upper view of HUIC 266, sample H4.

Fig. 22 *Palmatolepis quadrantinodosalobata* Sannemann, 1955: upper view of HUIC 267, sample H4.

Figs. 23-24 *Palmatolepis crepida* Sannemann, 1955: 23) upper view of HUIC 268, sample H5; 24) upper view of HUIC 269, sample H5.

Figs. 25-26 *Palmatolepis gracilis gracilis* Branson & Mehl, 1934: 25) upper view of HUIC 271, sample H9; 26) upper view of HUIC 272, sample T3.

Fig. 27 *Palmatolepis gracilis sigmoidalis* Ziegler, 1962: upper view of HUIC 273, sample H7.

Fig. 28 *Palmatolepis quadrantinodosa inflexa* Müller, 1956: upper view of HUIC 274, sample H6.

PLATE 2

All figures are x 40

Fig. 1 *Palmatolepis glabra prima* Ziegler & Huddle, 1969: upper view of HUIC 275, sample A.

Figs. 2-3 *Palmatolepis glabra pectinata* Ziegler, 1962: 2) upper view of HUIC 276, sample H6; 3) upper view of HUIC 277, sample H6.

Figs. 4-5 *Palmatolepis glabra distorta* Branson & Mehl, 1934: 4) upper view of HUIC 278, sample T2; 5) upper view of HUIC 279, sample H6.

Figs. 6-10 *Palmatolepis perlobata schindewolfi* Müller, 1956: 6) upper view of HUIC 283, sample H16; 7) upper view of HUIC 284, sample H19; 8) upper view of HUIC 280, sample D; 9) upper view of HUIC 281, sample B, 10) upper view of HUIC 282, sample B.

Fig. 11 *Palmatolepis perlobata* cf. *schindewolfi* Müller, 1956: upper view of HUIC 286, sample H13

Fig. 12 *Palmatolepis rugosa ampla* Müller, 1956: upper view of HUIC 287, sample H13.

Fig. 13 *Palmatolepis rugosa* cf. *ampla* Müller, 1956: upper view of HUIC 285, sample T2.

Fig. 14 *Palmatolepis glabra glabra* Ulrich & Bassler, 1926: upper view of HUIC 295B, sample H6.

Figs. 15-18 *Palmatolepis triangularis* Sannemann, 1955: 15) upper view of HUIC 291, sample H1; 16) upper view of HUIC 290, sample H2; 17) upper view of HUIC 292, sample H2; 18) upper view of HUIC 289, sample H2.

Fig. 19 *Palmatolepis tenuipunctata* Sannemann, 1955: upper view of HUIC 294, sample H5.

Fig. 20 *Palmatolepis subperlobata* Branson & Mehl, 1934: upper view of HUIC 270, sample H4.

Fig. 21 *Polygnathus glaber bilobatus* Ziegler, 1962: upper view of HUIC 296, sample B.

Fig. 22 *Polygnathus glaber medius* Helms & Wolska, 1967: upper view of HUIC 298, sample H6.

Fig. 23 *Polygnathus pseudobrevilaminus* Vorontsova, 1993: upper view of HUIC 305, sample H2.

Fig. 24 *Polygnathus brevilaminus* Branson & Mehl, 1934a: upper view of HUIC 303, sample H3.

PLATE 3

All figures are x 40

Figs. 1-5 *Polygnathus lanceolus* Vorontsova, 1993: 1, 2) upper and lower view of HUIC 306, sample H3; 3-4) upper, lateral and lower view of HUIC 307, sample H2.

Figs. 6-10 *Polygnathus communis* group Branson & Mehl, 1934a: 6, 7) upper and lower view of HUIC 309, sample H10; 8-10) upper, lateral and lower view of HUIC 310, sample E.

Figs. 11-12 *Polygnathus delicatulus* Ulrich & Bassler, 1926: upper and lower view of HUIC 311, sample H9.

Figs. 13-16 *Polygnathus semicostatus* Branson & Mehl, 1934: 13-15) upper, lateral and lower view of HUIC 312, sample E; 16) upper view of HUIC 313A, sample E.

Figs. 17-19 *Polygnathus ratebi* Yazdi, 1999: upper, lateral and lower view of HUIC 314, sample H2.

Figs. 20-22 *Polygnathus planirostratus* Dreesen & Dusar, 1974: upper, lateral and lower view of HUIC 315, sample A.

Figs. 23-25 *Polygnathus tichonovitchi* Kuzmin & Melnikova, 1991: upper, lateral and lower view of HUIC 316, sample H2.

Figs. 26-28 *Polygnathus nodocostatus* Branson & Mehl, 1934: 26) upper view of HUIC 316G, sample H3; 27) upper view of HUIC 318, sample H13; 28) lower view of HUIC 319, sample H4.

PLATE 4

All figures are x 40

Figs. 1-3 *Polygnathus subirregularis* Sandberg & Ziegler, 1979: 1) upper view of HUIC 320, sample B; 2-3) upper and lower view of HUIC 321, sample B.

Fig. 4 *Polygnathus perplexus* Thomas, 1949: upper view of HUIC 322, sample H7.

Fig. 5 *Polygnathus nodoundatus* Helms, 1961: upper view of HUIC 323, sample H13.

Figs. 6-9 *Polygnathus lagowiensis* Helms & Wolska, 1967: 6-7) upper and lower view of HUIC 326, sample H6; 8-9) upper and lower view of HUIC 325, sample A.

Figs. 10-14 *Polygnathus tenellus* Ji & Ziegler, 1993; 10-12) upper, lateral and lower view of HUIC 327, sample H2; 13-14) upper and lower view of HUIC 328, sample H3.

Figs. 15-17, 24, 26-27 *Polygnathus inconcinnus* Kuzmin & Melnikova, 1991: 15-16) upper, lateral and lower view of HUIC 329, sample A; 17) upper and lower view of HUIC 330, sample E; 24) upper view of HUIC 343, sample H4; 26-27) upper and lower view of HUIC 342, sample H3.

Figs. 18-23, 25 *Polygnathus yazdii* n. sp.: 18-20) upper, lateral and lower view of HUIC 331, sample H2; 21-23) upper, lateral and lower view of HUIC 334, sample B; 25) upper view of HUIC 332, sample H2.

Figs. 28-29 *Polygnathus* aff. *lagowiensis* Helms and Wolska, 1967: upper and lower view of HUIC 335, sample A.

PLATE 5

All figures are x 40

Figs. 1-16 *Polygnathus sardarensis* n. sp.: 1-2) upper and lower view of HUIC 337, sample H4; 3-4) oblique upper and lower view of HUIC 338, sample H4; 5-7) upper, lower and lateral view of HUIC 339, sample H4; 8-9)

upper and lower view of HUIC 348, sample H4; 10-11) upper and lower view of HUIC 341, sample H4; 12) upper view of HUIC 342, sample H3; 13) upper view of HUIC 343, sample H4; 14) upper view of HUIC 344, sample H4; 15-16) upper and lower view of HUIC 336, sample H3.

Fig. 17 *Polygnathus* sp. A: upper view of HUIC 345, sample H4.

Fig. 18 *Polygnathus* sp. B: upper view of HUIC 346, sample H5.

Fig. 19 *Polygnathus* sp. C: upper view of HUIC 347, sample H5.

Figs. 20-21 *Pseudopolygnathus primus* Branson & Mehl, 1934: 20) upper view of HUIC 235, sample H11; 21) upper view of HUIC 236, sample H11.

Fig. 22 *Pseudopolygnathus brevipennatus* Ziegler, 1962: upper view of HUIC 239, sample T3.

Fig. 23 *Pseudopolygnathus* sp.: upper view of HUIC 240, sample H7.

Figs. 24-27 *Bispathodus costatus* Branson, 1934: 24) upper view of HUIC 241, samples H10; 25) upper view of HUIC 242, samples H10; 26) upper view of HUIC 243, samples H10; 27) upper view of HUIC 244, samples H10.

PLATE 6

All figures are x 40

Fig. 1 *Bispathodus costatus* Branson, 1934: upper view of HUIC 245, sample H9.

Figs. 2-4 *Bispathodus aculeatus aculeatus* Branson & Mehl, 1934: 2) upper view of HUIC 248N, sample H10; 3) upper view of HUIC 246, sample H9; 4) upper view of HUIC 247, sample H11.

Figs. 5-7 *Bispathodus stabilis* Branson & Mehl 1934: 5) upper view of HUIC 250, sample D; 6) upper view of HUIC 251, sample H19; 7) upper view of HUIC 255, sample D.

Figs. 8-11 *Alternognathus beulensis* Ziegler & Sandberg, 1984: 8-9) upper and lower view of HUIC 237, sample H7; 10-11) upper and lower view of HUIC 238, sample H7.

Fig. 12 *Clydagnathus* sp.: upper view of HUIC 256, sample H19.

Fig. 13 *Branmehla inornata* Branson & Mehl 1934: upper view of HUIC 249, sample H10.

Fig. 14 *Mehlina* sp.: lateral view of HUIC 248O, sample T3.

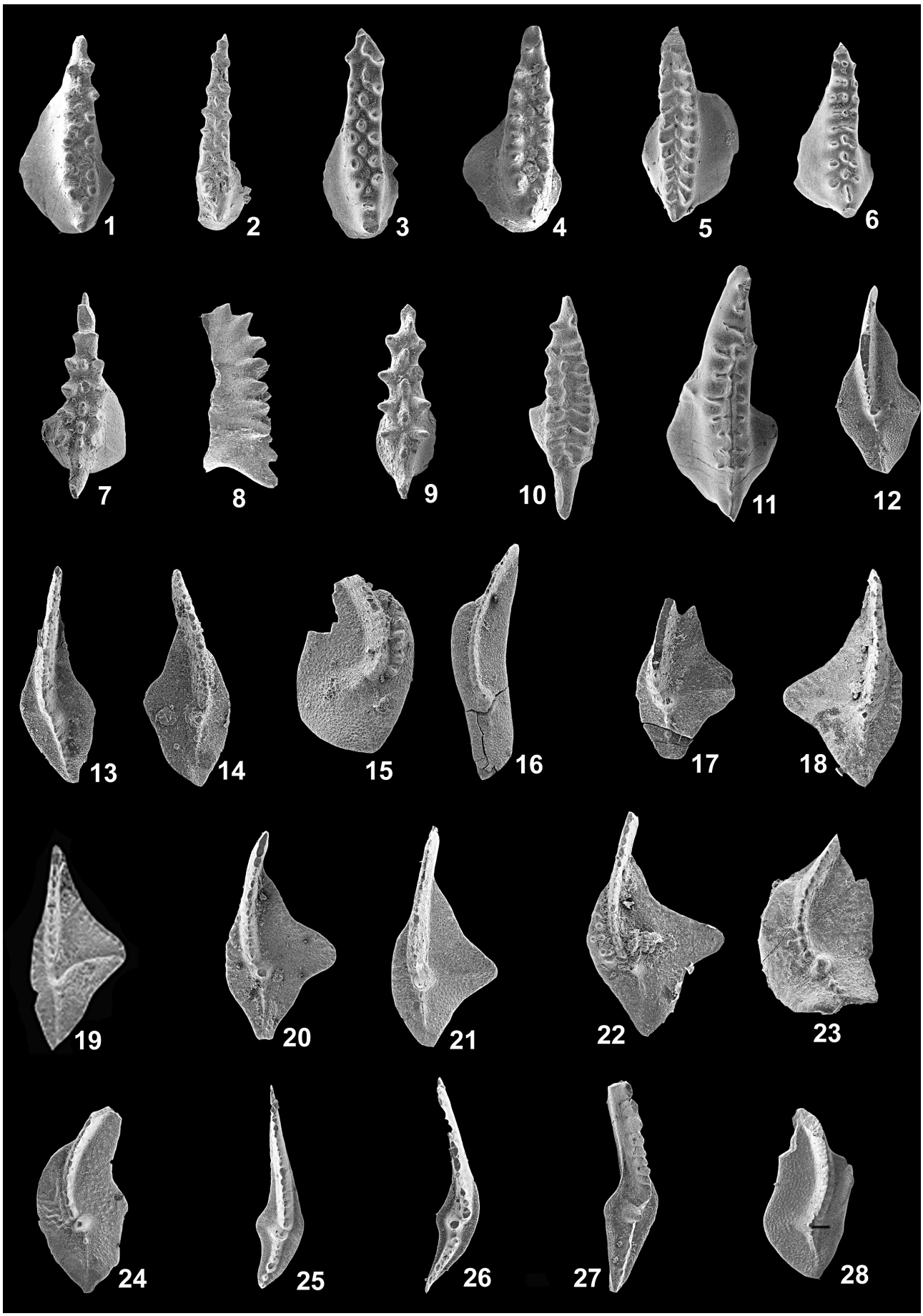

PLATE 1

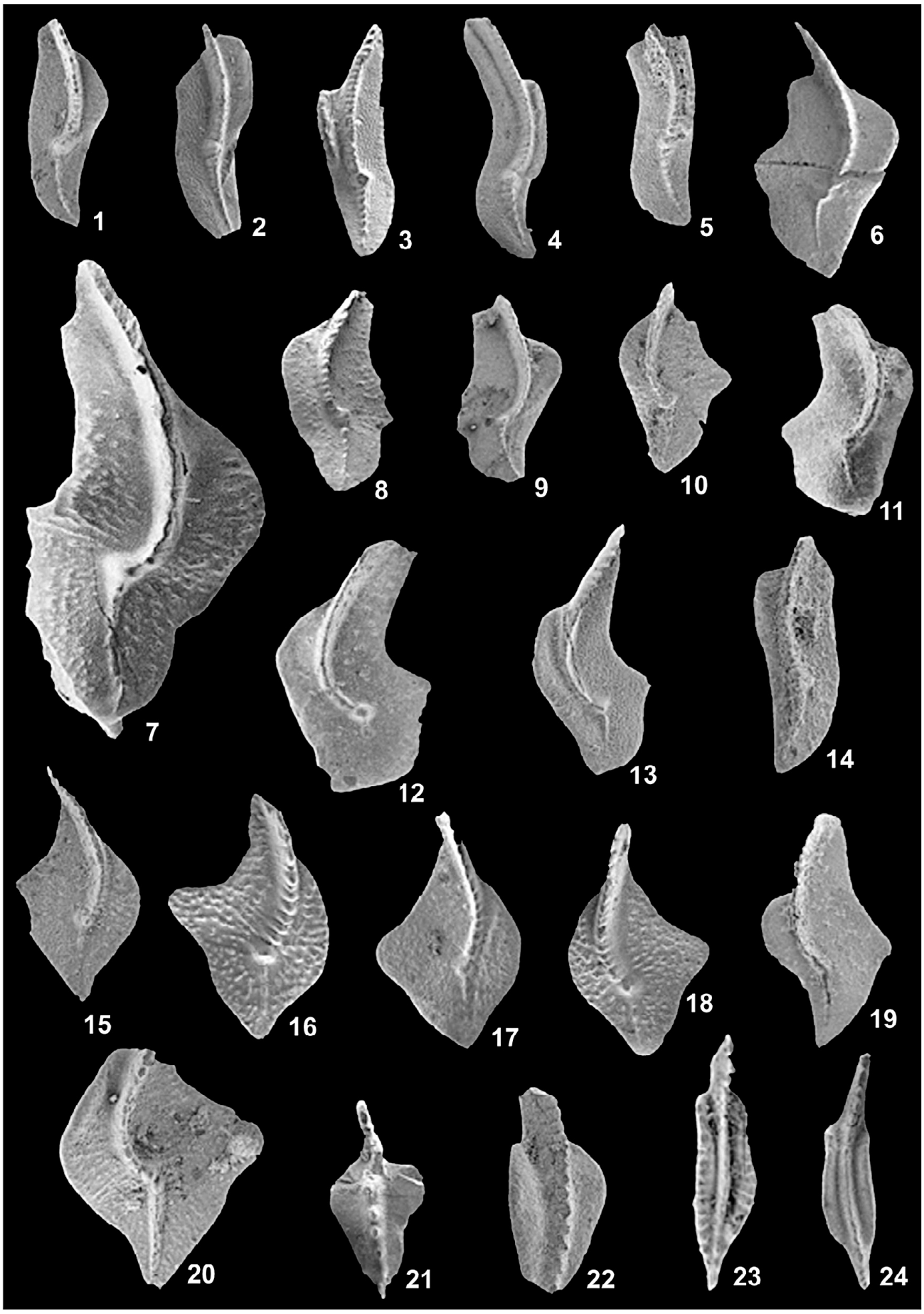

PLATE 2

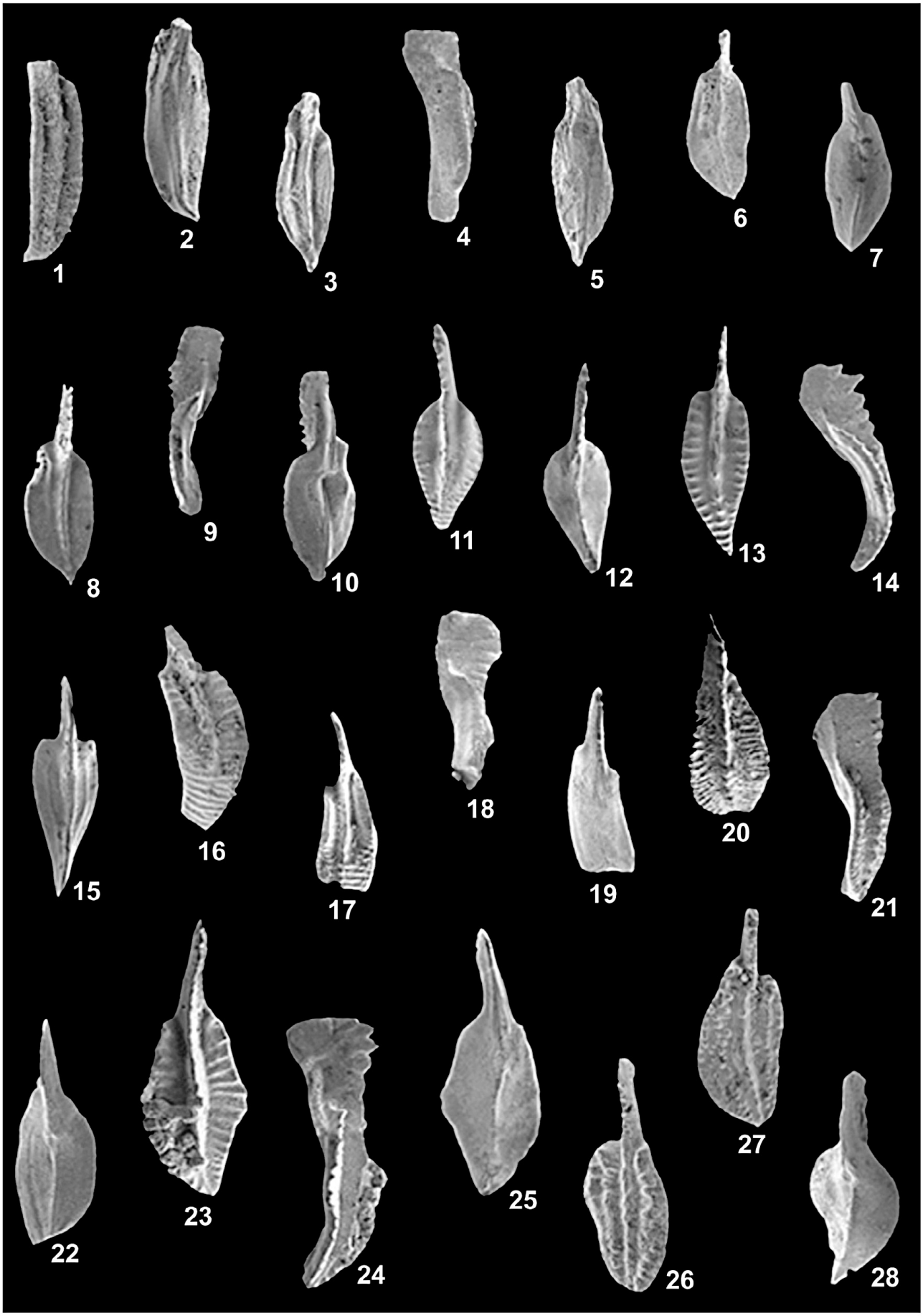

PLATE 3

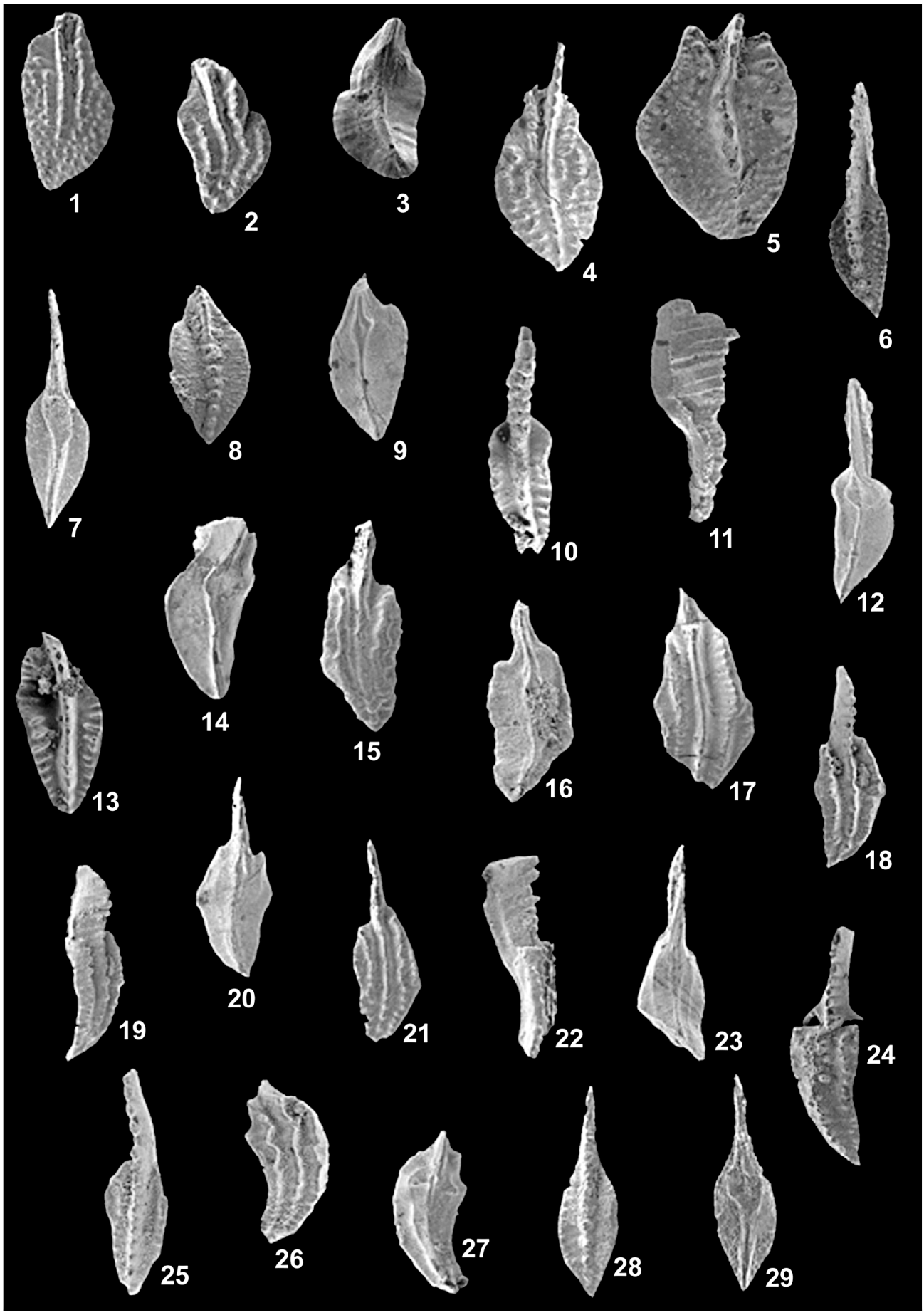

PLATE 4

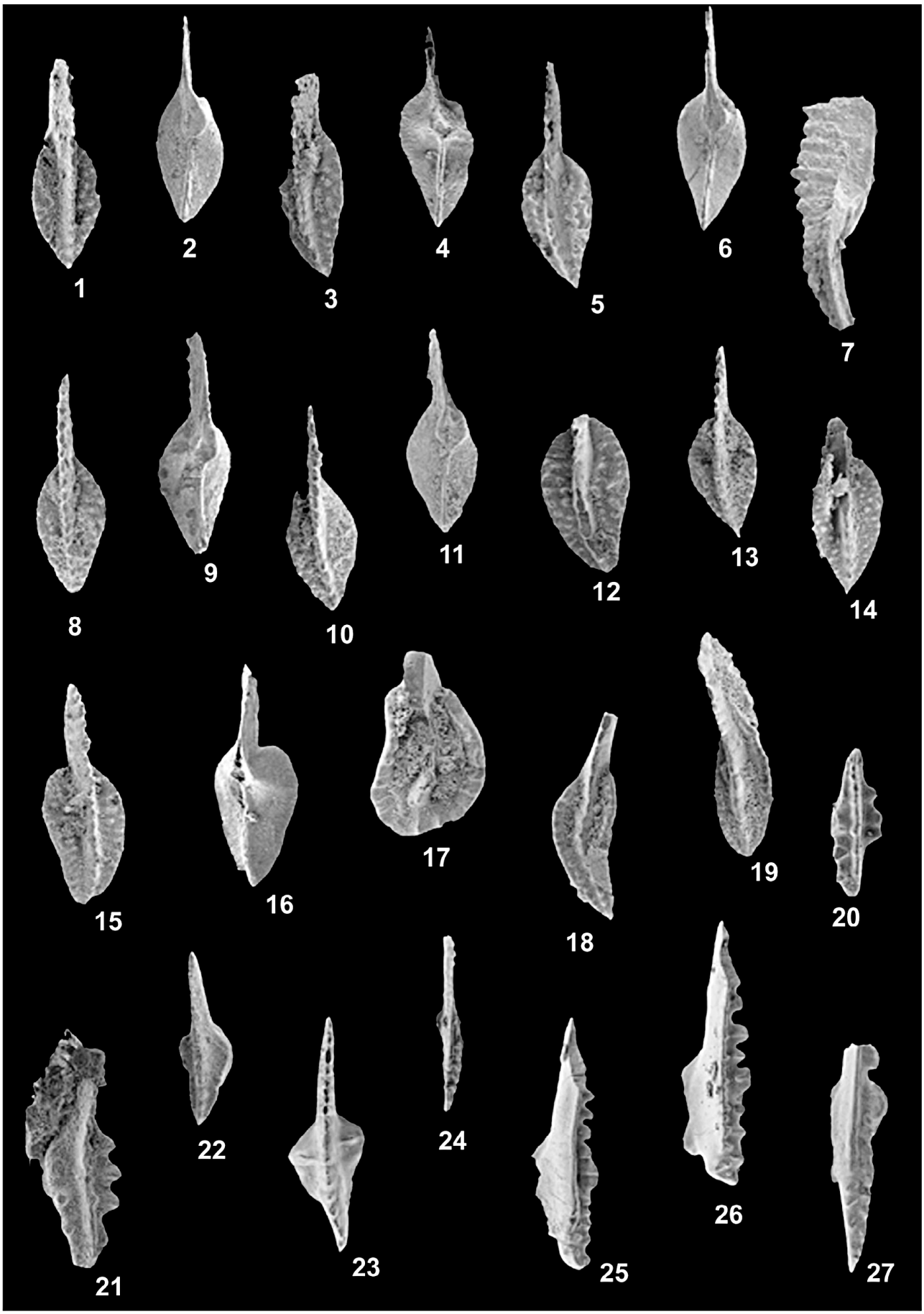

PLATE 5

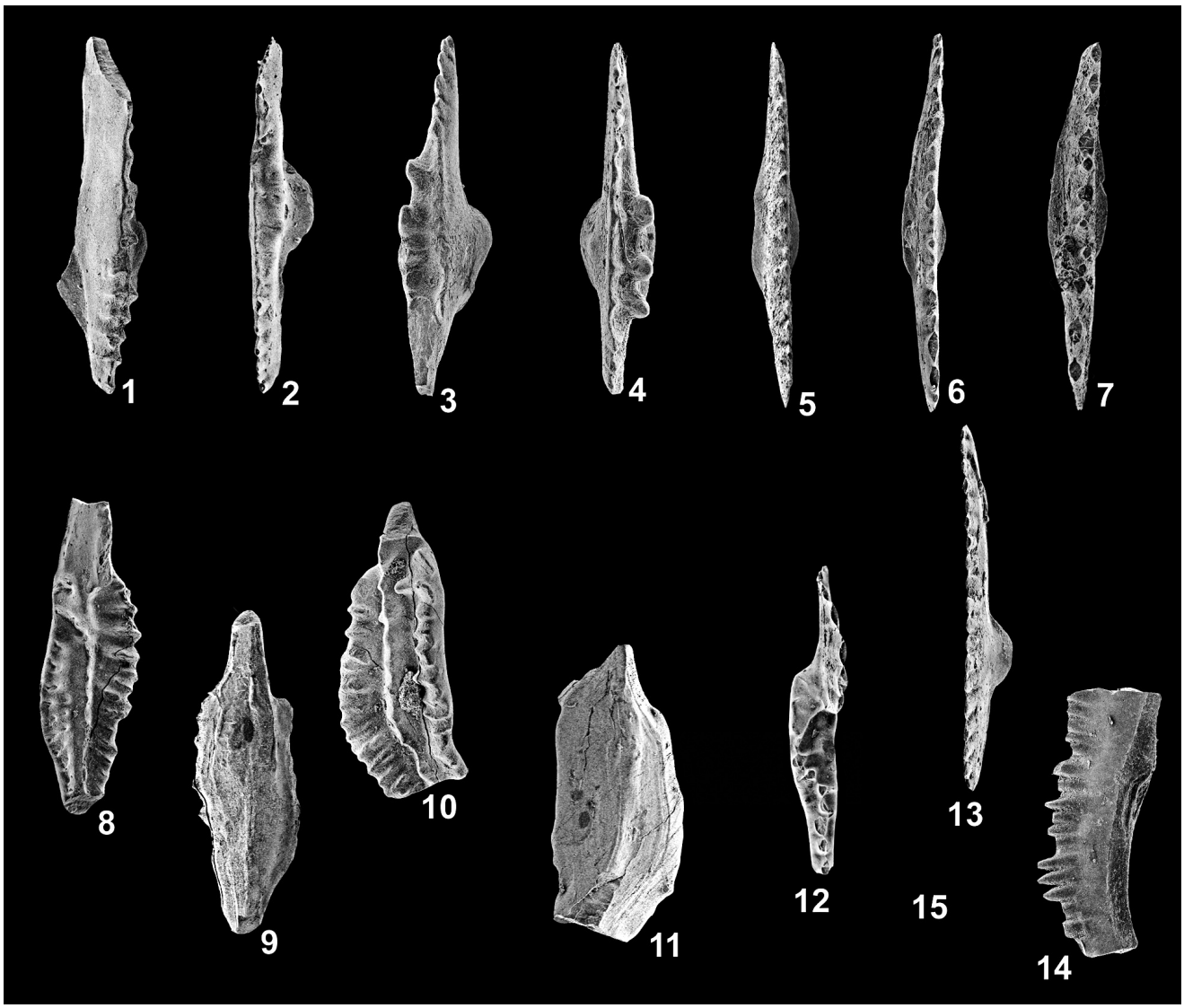

PLATE 6

REFERENCES

Ashouri A.R. (2002) - *Palmatolepis* (Conodonta; Late Devonian) from Tabas region, eastern Iran. *Iran. Int. J. Sci*., 3: 187-220, Tehran.

Ashouri A.R. (2004) - Late Devonian and Middle - Late Devonian conodont from eastern and northern Iran. *Riv. Esp. Micropaleont*., 36: 355-365, Madrid.

Ashouri A.R. & Yamini A. (2006) - Cephalopods and stratigraphical position of Cephalopod Bed of Shishtu Formation, Iran. *Geosci. Scient. Quart. J.,* 15(60): 178-187.

Barskov I.S., Alekseev A.S., Kononova L.I. & Migdisova A.V. (1987) - Atlas of Upper Devonian and Carboniferous conodonts. V. of 144 pp. Moskovskiy Gosudarstvennyy Univ., Moscow.

Barskov I.S., Vorontsova T.N., Kononova L.I. & Kuzmin A.V. (1991) - Oprdelitel konodontov devona i nizhnego karbona. V. of 183 pp. Moskovskiy Gosudarstvennyy Univ., Moscow.

Becker R.T., Ashouri A.R. & Yazdi M. (2004) - The Late Devonian Annulata event in the Shotori Range (eastern Iran). *N. Jb. Geol. Paläont. Abbh*., 231: 119-143, Stuttgart.

Capkinoglu S. (1997) - Conodont fauna and biostratigraphy of Famennian of Buyukada, Istanbul, northwestern Turkey. *Boll. Soc. Paleont. Ital.*, 35(2): 165-185, Modena.

Feist R., Yazdi M. & Becker R.T. (2003) - Famennian trilobites from the Shotori Range, E-Iran. *Ann. Soc. Géol. Nord,* 10: 285-295, Lille.

Gholamalian H. (2006) - Biostratigraphy of Late Devonian sequence in Hutk section (north of Kerman) based on conodonts. *Geosci. Quart. J.,* 15(59): 94-101, (in Persian with English abstract), Tehran.

Gholamalian H. (2007) - Conodont biostratigraphy of the Frasnian-Famennian boundary in the Esfahan and Ta-

bas areas, Central Iran. *Geol. Quar.*, 51(4): 453-476, Warszawa.

Gholamalian H. & Kebriaei M.R. (2008) - Late Devonian conodonts from the Hojedk section, Kerman Province, southeastern Iran. *Riv. It. Paleont. Strat.*, 114(2): 171-181, Milano.

Hairapetian V. & Yazdi M. (2003) - Late Devonian conodonts from Dalmeh section, northeastern Ardekan, Central Iran. *Cour. Forsch. Senckenberg*, 245: 209-225, Frankfurt.

Ji Q. & Ziegler W. (1993) - The Lali section: an excellent reference section for Late Devonian in south China. *Cour. Forsch. Senckenberg*, 157: 183 pp., Frankfurt.

Klapper G. (2007) - Frasnian (Upper Devonian) conodont succession at House Spring and correlative sections, Canning Basin, Western Australia. *J. Palaeont.*, 81(3): 513-537, Lawrence.

Klapper G., Feist R., Becker R.T. & House M.R. (1993) - Definition of the Frasnian/ Famennian stage boundary. *Episodes*, 16: 433-441, Beijing.

Klapper G., Uyeno T., Armstrong D.K. & Telford P.G. (2004) - Conodonts from the Willams Island and Long Rapids formations (Upper Devonian, Frasnian - Famennian) of the Onakawana B drillhole, Moose River Basin, northern Ontario, with a revision of Lower Famennian species. *J. Palaeont.*, 78(2): 371-387, Lawrence.

Kuzmin A.V. & Melnikova L.I. (1991) - Novyye rannefamenskyye konodonty. *Paleont. Zhur.*, 1: 123-128, Moscow.

Perri M.C. & Spalletta C. (1990) - Famennian conodonts from climenid pelagic limestone, Carnic Alps, Italy. *Palaeontographica Italica*, 77: 55-83, Pisa.

Pohler S.M. & Barnes C.R. (1990) - Conceptual models in conodont paleoecology. *Cour. Forsch. Senckenberg*, 118: 409-440, Frankfurt.

Sandberg C.A. & Dreesen R. (1984) - Late Devonian icriodontid biofacies models and alternate shallow water conodont zonation. In: Clark D.L. (Ed.) - Conodont biofacies and provincialism. *Geol. Soc. America Spec. Pap.*, 196: 143-178, Boulder.

Sandberg C.A., Ziegler W., Dreesen R. & Butler J. (1988) - Late Frasnian mass extinction. Conodont event stratigraphy, global changes and possible causes. *Cour. Forsch. Senckenberg*, 102: 263-307, Frankfurt.

Savoy L. E. & Harris A.G. (1993) - Conodont biofacies and taphonomy along a carbonate ramp to black shale basin (latest Devonian and earliest Carboniferous), southestern Canadian Cordillera and adjacent Montana. *Canad. J. Earth Sci.*, 30: 2404-2422, Calgary.

Schülke I. (1995) - Evolutive prozesse bei *Palmatolepis* in der frühen Famenne-Stuffe (Conodonta, Ober-Devon). *Göttinger Arb. Geol. Paläont.*, 67: 1-108, Göttingen..

Stöcklin J., Eftekhar-nezhad J. & Hushmandzadeh A. (1965) - Geology of Shotori Range (Tabas area, east Iran). *Geol. Survey Iran, Reports*, 3: 69 pp., Tehran.

Walliser O.H. (1966) - Devonian and Carboniferous goniatites in Iran, contribution to the Palaeontology of East Iran. *Geol. Surv. Iran, Reports*, 6: 57 pp., Tehran.

Wendt J., Kaufmann B., Belka Z., Farsan N. & Karimi Bavandpour A. (2002) - Devonian/Lower Carboniferous stratigraphy, facies patterns and palaeogeography of Iran, part I, southeastern Iran. *Ac. Geol. Polonica*, 52(2): 129-168, Warszawa.

Wendt J., Kaufmann B., Belka Z., Farsan N. & Karimi Bavandpour A. (2005) - Devonian/Lower Carboniferous stratigraphy, facies patterns and palaeogeography of Iran, part II, northern and central Iran. *Ac. Geol. Polonica*, 55(1): 31-97, Warszawa.

Yazdi M. (1999) - Late Devonian - Carboniferous conodonts from eastern Iran. *Riv. It. Paleont. Strat.*, 105: 167-195, Milano.

Yazdi M., Meysami A., Mannani M., Bakhshaei M.H. & Mawson R. (2000) - Famennian conodonts from the Esteghlal Refractories Mine, Abadeh area, south-central Iran. *Rec. West. Austral. Mus. Suppl.*, 58: 197-209, Perth.

Ziegler W. (1962) - Phylogenetische Entwicklung strtigraphisch wichtiger conodonten - gattungen in der *Manticoceras* stufe (Oberdevon, Deutschland). *N. Jb. Geol. Paläont. Abh.*, 114(2): 142-168, Stuttgart.

Ziegler W. & Sandberg C.A. (1984) - *Palmatolepis*-based revision of upper part of standard Late Devonian conodont zonation. *Geol. Soc. America, Spec. Pap.*,196: 179-194, Denver.

Ziegler W. & Sandberg C.A. (1990) - Late Devonian standard conodont zonation. *Cour. Forsch. Senckenberg*, 121: 115 pp., Frankfurt.

Ziegler W., Sandberg C.A. & Austin R.L. (1974) - Revision of *Bispathodus* group (Conodonta) in the Upper Devonian and Lower Carboniferous. *Geologica et Palaeontologica*, 8: 97-112, Marburg.